e-Polymers **2007**, no. 011 http://www.e-polymers.org
ISSN 1618-7229

Self-Assembly of Methacrylic Nanostructured Copolymers Containing Polyhedral Oligomeric Silsesquioxanes

D. Molina,[1] *M. Levi*,[1] *S. Turri*,[1]* *M. Penso*[2]

[1] Dipartimento di Chimica, Materiali e Ingegneria Chimica "G. Natta", Politecnico di Milano, Piazza L. da Vinci 32, 20133, Milano, Italy, *e-mail: stefano.turri@polimi.it
[2] Istituto di Scienze e Tecnologie Molecolari, CNR, Via Golgi 19, 20133, Milano, Italy.

(Received: 26 October, 2006; published: 26 January, 2007)

Abstract: Two hybrid copolymer series obtained by free-radical copolymerization of methacrylcyclohexyl Polyhedral oligomeric silsesquioxane (POSS) with butyl methacrylate or 2-ethylhexylmethacrylate were characterized by ^{1}H-NMR spectroscopy, gel permeation chromatography (GPC), X-rays Diffraction (XRD), differential scanning calorimetry (DSC) and thermo-gravimetric analysis (TGA). Reactivity ratios were calculated by low yield composition data suggesting the formation of random copolymers with low probability of poly-POSS sequences. XRD studies showed the crystallization behaviour of the inorganic phase independently on the POSS content; however sample processing by solvent casting effectively hindered the copolymer self-assembling ability. DSC suggests the formation of polyphasic structures with T_g increasing with POSS content, and with endothermal peaks occurring at higher temperature. Finally TGA shows an improved thermal stability of hybrid copolymers with char yield correlated to the level of inorganic phase.

Introduction

Hybrid copolymers containing Polyhedral oligomeric silsesquioxanes (POSS) represent an innovative class of nanostructured materials; several reviews have appeared on this topic during the last 8 years. [1-5].

POSS are molecular nanoparticles consisting of a cubic Si_8O_{12} cage of nanometric size, bearing at its corners eight organic groups. The choice of such groups can affect both solubility as well as chemical reactivity. Actually, in contrast to the majority of nanoparticles, reactive POSS can be used as a building blocks in various types of polymerization processes: examples of functionalities available include [1] hydroxyl, epoxy, carboxyl, vinyl, acrylate or methacrylate, silanol and some others. Thanks to covalent binding between organic matrix and inorganic nanoparticle, a control at molecular level of the macromolecular architecture is feasible. In light of this, a wide array of both thermoplastics and thermosetting materials have been modified [3] by copolymerization or grafting with reactive POSS. It has been claimed that many physical properties of the polymer can be significantly improved, like typically the elastic modulus, T_g, thermal stability, fire resistance and, more recently, surface properties like decreased wettability [6].

POSS nanoparticles are highly crystalline. X-rays Diffraction studies [7] showed that they self-assemble to form a hexagonally packed structure. How this morphology changes or is retained in POSS containing hybrids is dependent on the affinity between the host polymer and POSS substituents. For example, it has been reported

that introduction of POSS in an inherently amorphous architecture, like a methacrylic random copolymer, completely suppresses its crystallization behaviour [8]. By contrast, in other cases, ordered, self-assembled hybrid structures were found in polystyrene [9], polynorbornene [10], polyurethanes [11], polybutadiene [12] and even when host matrices were crystallizable like in case of polyethylene [13, 14]. The nature of the obtained nanostructure, whether amorphous or crystalline, has a significant effect also on physical properties of the hybrid material like its stiffness or thermal stability.

Among the various compositions, acrylic and methacrylic copolymers have been described and obtained by free radical [8] and atom transfer radical polymerization processes [15]. Some applications were also envisaged as resist materials [16]. In this article two series of methacrylic copolymers based on low T_g, inherently amorphous monomers like butylmethacrylate and 2-ethylhexylmethacrylate have been prepared in a very wide composition range. Their structures were studied through XRD and by thermal characterization techniques in order to assess the self-assembling behaviour of the obtained hybrid copolymers.

Results and discussion

The chemical structures of monomers used are shown in Figure 1. The corresponding hybrid addition copolymers made of the monomer pairs (a+b) and (a+c) will be indicated subsequently as BU-POSS and EE-POSS respectively.

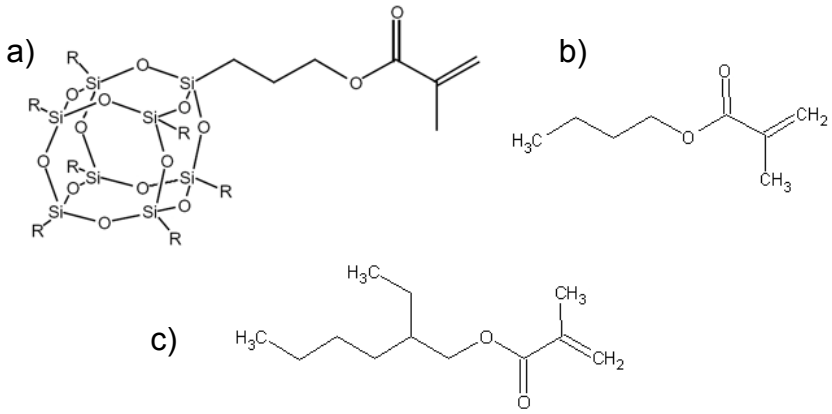

Fig. 1. Structure of cyclohexyl methacryloyl propyl polyhedral silsesquioxane POSS (a), Butyl methacrylate (b), 2-ethylhexyl methacrylate (c), R = cyclohexyl.

Composition of the two copolymer series (a+b and a+c) was investigated through ^1H NMR spectroscopy. Some examples of spectra obtained are shown in Figure 2. This analysis confirms the absence of free POSS macromonomer in the purified copolymer (signals at 5.5 ppm, 6.1 ppm are not present in copolymer), as revealed also by GPC characterization. Tables 1 and 2 report composition, relative M_w (weight average molecular weight) by GPC, and yield for BU-POSS and EE-POSS copolymers. The M_w and the polydispersity trend is not clear, however the number average polymerization degree Xn is significantly decreasing with the POSS content as shown in Figure 3, suggesting a lower reactivity of the hybrid macromonomer. The

upper three copolymers reported in Table 1 are characterized by low PDI values possibly because of some fractionation effect during purification, as suggested also by their lower yields.

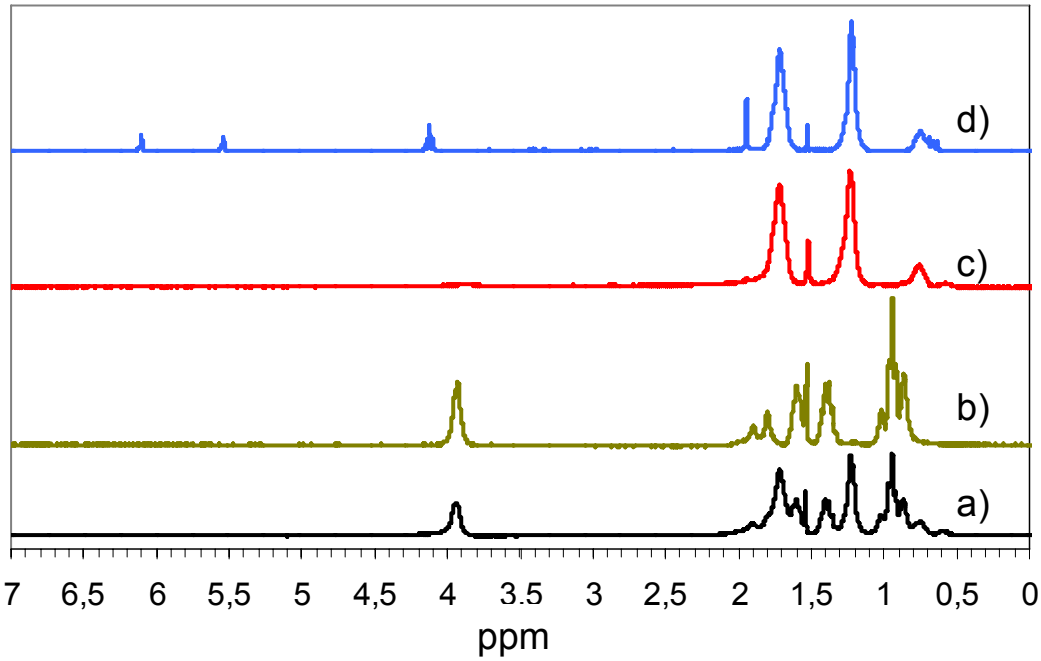

Fig. 2. ^{1}H-NMR spectrum of BU-POSS 5 (see Table 1 for details) copolymer (- a), polybutylmethacrylate homopolymer (- b), POSS homopolymer (- c) and POSS monomer (- d).

Tab. 1. Summary of molecular weight and composition data of BU-POSS copolymers.

Sample	POSS in feed (wt%)	POSS in copolymer (wt%)	Mw	PDI	Yield (wt%)
Buma*	0	0	242	1,3	50,2
BU-POSS 1	10	10	221	1,3	40,5
BU-POSS 2	20	18	207	1,3	41,2
BU-POSS 3	30	28	173	1,5	58,0
BU-POSS 4	40	40	162	1,9	77,9
BU-POSS 5	50	43	180	2,6	88,6
BU-POSS 6	60	55	187	2,6	64,0
BU-POSS 7	70	67	295	2,5	73,2
BU-POSS 8	80	71	260	2,4	72,9
BU-POSS 9	90	83	264	1,7	80,0

*Buma = Poly(butyl methacrylate)

In order to calculate the reactivity ratios r_1 and r_2 of the butyl methacrylate-methacrylcyclohexyl POSS pair, a series of polymerization runs at low yield (≤8 wt %)

were carried out, reducing the reaction time from 24h to 20 minutes. Results are collected in Table 3.

Tab. 2. Summary of molecular weight and composition data of EE-POSS copolymers.

Sample	POSS in feed (wt%)	POSS in copolymer (wt%)	Mw	PDI	Yield (wt%)
Eema*	0	0	151	2,2	89,2
EE-POSS 1	10	10	119	2,6	80,2
EE-POSS 2	20	19	116	2,5	85,1
EE-POSS 3	30	30	152	3,1	88,2
EE-POSS 4	40	36	183	2,5	89,5
EE-POSS 5	50	46	104	2,4	91,3
EE-POSS 6	60	51	246	2,4	88,3
EE-POSS 7	70	67	349	2,4	83,9
EE-POSS 8	80	75	215	3,8	74,6
EE-POSS 9	89	83	237	4,8	66,5

*Eema = 2-ethylhexyl methacrylate homopolymer

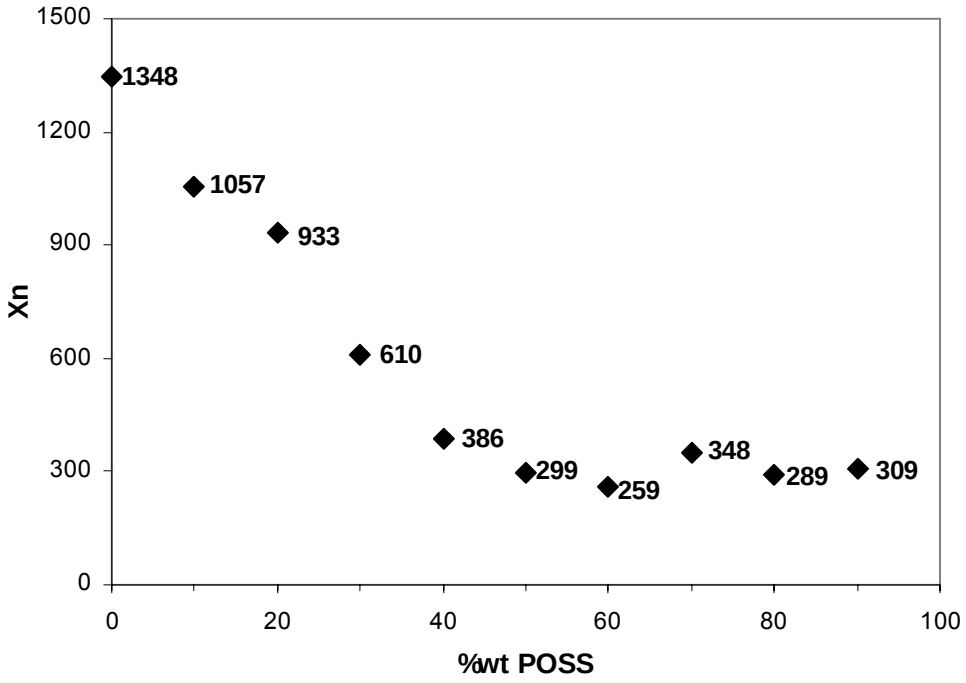

Fig. 3. Number Average degree of polymerization of BU-POSS copolymer series vs POSS content.

After NMR analysis a calculation of molar fractions were done, and reactivity ratios were computed by least square fitting of low yield composition data according to one of the classical relations shown below [17-19].

The Mayo-Lewis equation:

$$F_1 = \frac{r_1 f_1^2 + f_1 f_2}{r_1 f_1^2 + 2 f_1 f_2 + r_2 f_2^2} \quad (1)$$

where f_1 and f_2 are the molar fraction of monomer in feed, F_1 and F_2 are the molar fraction of monomer in the copolymer and where r_1 and r_2 are the kinetic constant s ratio of copolymer reactions. This equation can be linearized in the following form,

$$x\left(1-\frac{1}{n}\right) = r_1 \frac{x^2}{n} - r_2 \quad (2)$$

where x is the ratio between f_1 and f_2 and where n is the ratio between F_1 and F_2.

The Fineman- Ross equation:

$$G = r_1 H - r_2 \quad (3)$$

where $G = x\frac{n-1}{n}$ and $H = \frac{x^2}{n}$.

The inverted Fineman-Ross equation:

$$\frac{G}{H} = -r_2\left(\frac{1}{H}\right) + r_1 \quad (4)$$

and the Kelen Tudos equation:

$$\eta = \left(r_1 + \frac{r_2}{\alpha}\right)\zeta - \frac{r_2}{\alpha} \quad (5)$$

where $\alpha = \sqrt{H_{max} H_{min}}$, $\zeta = \frac{H}{\alpha + H}$ and $\eta = \frac{G}{\alpha + H}$.

Accordingly, Table 4 summarizes the reactivity ratios r_1, r_2 and the correlation coefficients of the linear regressions obtained from equations 2,3,4,5.

Tab. 3. Summary of molecular weight and composition data of BU-POSS copolymers obtained at low yield.

Sample (polymerization time)	Yield (wt%)	POSS in feed (%wt)	POSS in copolymer (%wt)
BU-POSS 1 (20 min)	6,96	10	8
BU-POSS 3 (20 min)	8,18	30	25
BU-POSS 5 (20 min)	6,97	50	42
BU-POSS 7 (20 min)	5,25	69	61

Tab. 4. Reactivity ratios from butyl methacrylate – methacrylcyclohexyl POSS low yield copolymerizations.

Method	POSS reactivity ratio	BUMA reactivity ratio	R^2
Mayo Lewis	0,22	1,29	0,9537
Fineman Ross	0,22	1,29	0,9537
Inverted Fineman Ross	0,35	1,30	1,0000
Kelen Tudos	0,27	1,30	0,9998

All Table 4 data are in quite good agreement with each other suggesting that POSS macromonomer has a reactivity ratio much less than unity in contrast to butyl methacrylate. This difference in reactivity seems reasonable due to the strong difference in molecular size and steric hindrance between the two monomers. Therefore the macromolecular body should consist in a random copolymer with longer butyl methacrylate sequences and insertion of some isolated POSS units.

By knowing r_1 and r_2 it is feasible to draw the composition diagram F_1-f_1. The F_{POSS} – f_{POSS} plot is shown in Figure 4 in the case of the inverted Fineman-Ross method. Low yield data come from Table 3 while high yield points correspond to Table 1 data. It can be observed that the extrapolated composition curve fits quite well the experimental points.

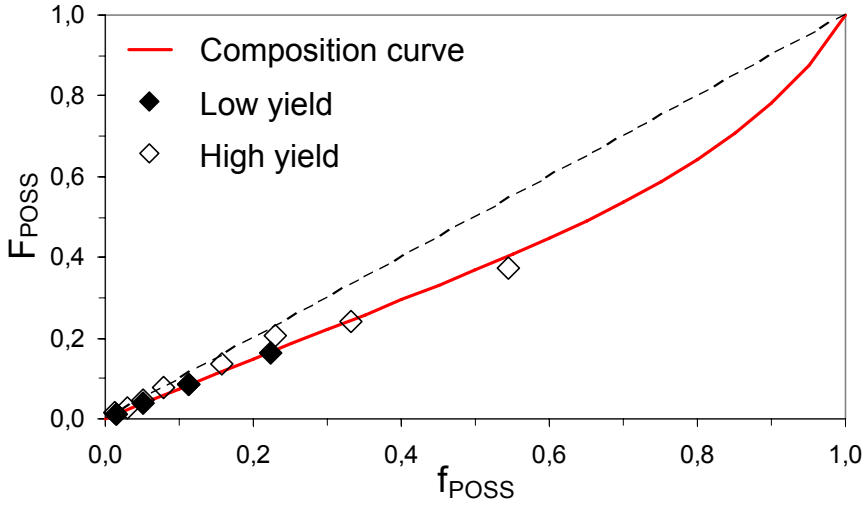

Fig. 4. Composition curve of low yield BU-POSS series.

The XRD patterns of BU-POSS copolymers are shown in Figures 5 (lower POSS content) and 6 (higher POSS content). It should be underlined that the former samples were prepared by solvent casting techniques (Figure 5, see experimental) since they show good solubility and they cannot be powdered due to their high toughness. On the other hand the higher POSS level samples could not form a homogeneous film by casting since it's too brittle, but they could be easily analyzed in form of powder. Interestingly samples *f* and *g* shown in Figure 5, and samples *a* and *b* in Figure 6 are exactly the same copolymers at intermediate POSS content processed in two ways. Samples in Figure 5 show absence of crystallinity in contrast to the starting POSS macromonomer. These hybrids are characterized by two amorphous halos centered at 2θ = 7.2° and 18.8°, with minor differences with respect to poly(butyl methacrylate) homopolymer. In this case the random copolymerization process prevents crystallization of the dispersed silsesquioxane cages, like reported for other methacrylic hybrid copolymers [8].

Figure 6 shows the XRD patterns of methacrylcyclohexyl POSS in comparison to powders made of BU-POSS copolymers with a high content of silsesquioxane. The nanofiller shows sharp reflections at 2θ = 7.83°, 10.46°, 11.61°, 18.14°, 18.80°. The XRD analysis of POSS copolymers in Figure 6 shows the reflection at 2θ=7.2°, rather sharp and not too far from 101 reflection of POSS monomer, suggesting the formation of a crystalline order in the hybrid copolymer. The different behaviour

observed in Figure 5 and 6 could be attributed to an easier self-assembly of silsesquioxane cages in POSS rich copolymers, strongly affected by the sample processing conditions. Qualitatively, the same consideration holds for EE-POSS series (data not shown).

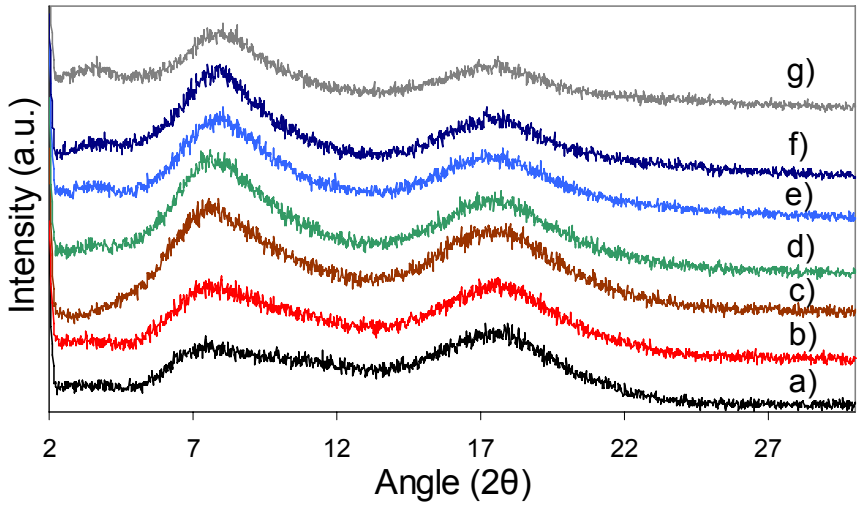

Fig. 5. X-Ray diffraction profiles of BU-POSS copolymer films obtained from solvent solution: polybutylmethacrylate homopolymer (- a), BU-POSS 1 (- b), BU-POSS 2 (- c), BU-POSS 3 (- d), BU-POSS 4 (- e), BU-POSS 5 (- f) and BU-POSS 6 (- g) (for composition see Table 1).

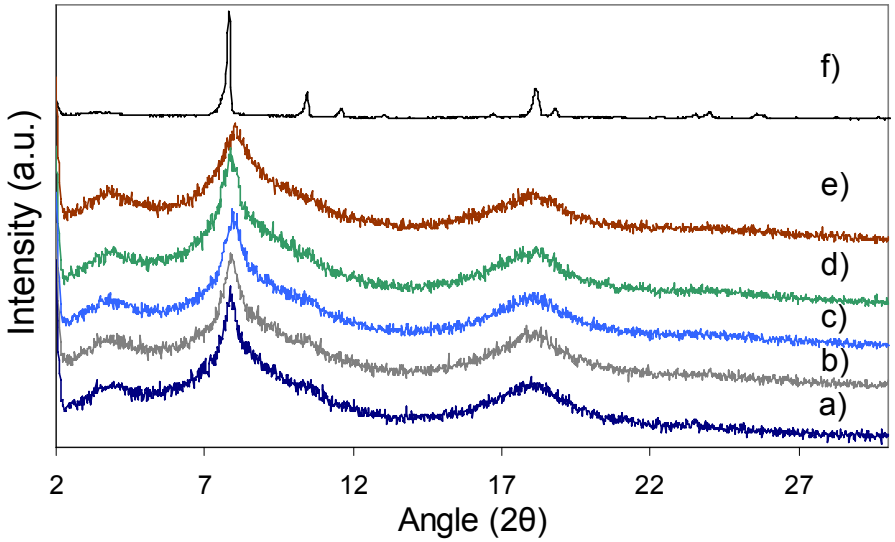

Fig. 6. X-Ray diffraction profiles of BU-POSS copolymer powders: BU-POSS 5 (- a), BU-POSS 6 (- b), BU-POSS 7 (- c), BU-POSS 8 (- d), BU-POSS 9 (- e) and methacrylcyclohexyl polyhedral oligomeric silsesquioxane (POSS) (- f) (for composition see Table 1).

By analogy with other systems [12], the crystal aggregation of POSS cages can be constrained by their covalent attachment to the macromolecular chain, forming a bidimensional structure where silsesquioxanes maintain their hexagonal symmetry.

Crystal size of the copolymers in the 101 direction can be estimated by the Scherrer formula (equation 11) analyzing the most intense reflection at $2\theta=7.2°$

$$L = (k\,\lambda)/(\beta_{hkl}\cos\theta) \quad (11)$$

where β_{hkl} is the half-height width of the hkl indexed reflection, θ = diffraction angle, λ = wavelength of radiation source, and k is a constant close to unity. Results concerning high POSS level powders are reported in Table 5 for both copolymer series. It appears that crystal growth is inhibited by copolymerization especially in case of 2-ethylhexylmethacrylate. Moreover increasing the POSS content further decrease the crystal size possibly because of the reduced molecular mobility of the chain.

Tab. 5. Crystal size in POSS copolymers according to the Scherrer formula.

Sample	L (Å)
Methacrylcyclohexyl POSS	702
EE-POSS 5	65.7
EE-POSS 6	73.8
EE-POSS 7	89.7
EE-POSS 8	44.4
EE-POSS 9	42.5
BU-POSS 5	102.1
BU-POSS 6	102.2
BU-POSS 7	102.7
BU-POSS 8	104.2
BU-POSS 9	63.3

Comparison between BU-POSS 5 and BU-POSS 6 hybrids in Figures 5 and 6 clearly shows the strong effect of processing conditions on the self-assembling ability of POSS based copolymers. Solution casting and following fast evaporation procedure completely inhibits self-assembly of POSS units from the amorphous host matrix. Similarly, a negative effect of solvent on crystallization was reported by Waddon et al. [13] in case of hybrids with crystalline host matrix.

To shed further light on BU-POSS and EE-POSS copolymer structures, thermal analysis was carried out by DSC showing a progressive copolymer T_g increase with the POSS content. Experimental data were fitted according to classical relations like Fox equation [20] and Johnston equation [21] but with very poor results. As shown in Figure 7 a better interpolation of T_g data for BU-POSS series was obtained through the Couchman-Karasz [22] equation:

$$\ln(T_g)=\frac{\ln(T_{g1})+h\frac{w_2}{w_1}\ln(T_{g2})}{1+h\frac{w_2}{w_1}} \quad (12)$$

where h was considered as an adjustable parameter and temperatures are in Kelvin. However equation 12 leads to an extrapolated T_g value of about 390-400 K, while it is

known that poly-POSS homopolymers generally decompose before softening at T > +673 K [8, 23].

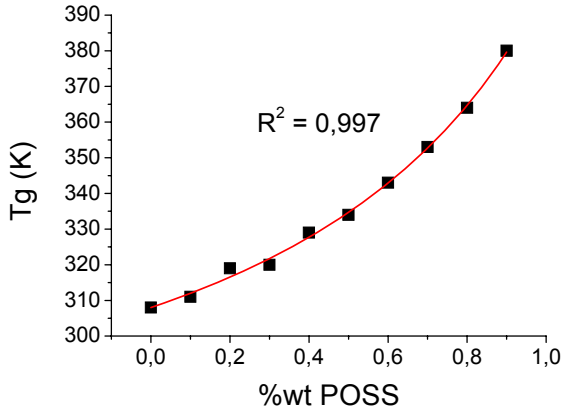

Fig. 7. T_g – composition curve in BU-POSS copolymers according to Couchman-Karasz equation.

One possible explanation of this is the fact that such hybrid copolymers, or at least those at higher nanofiller content, are not truly monophasic as also suggested by XRD analysis. Actually at T > + 150°C in copolymers with POSS content higher than 40% wt, some endothermic relaxations or melting peaks occur (Figure 8) at increasing temperatures with silsesquioxane content. These phenomena are obvious in first scan, but in second scan after a rapid quenching cycle such peaks disappear (data not shown) and leave a broad, progressive heat capacity change not easy to be quantified. It could be concluded that quenching cycle, as well as solvent evaporation procedure, effectively hinder the self-assembling ability of POSS phase. Similar behaviours were described in literature: Pyun et al. [24] in a recent study concerning silsesquioxane based block copolymers found endothermal peaks at T > T_g which were attributed to enthalpy relaxations correlated to physical aging of the POSS phase.

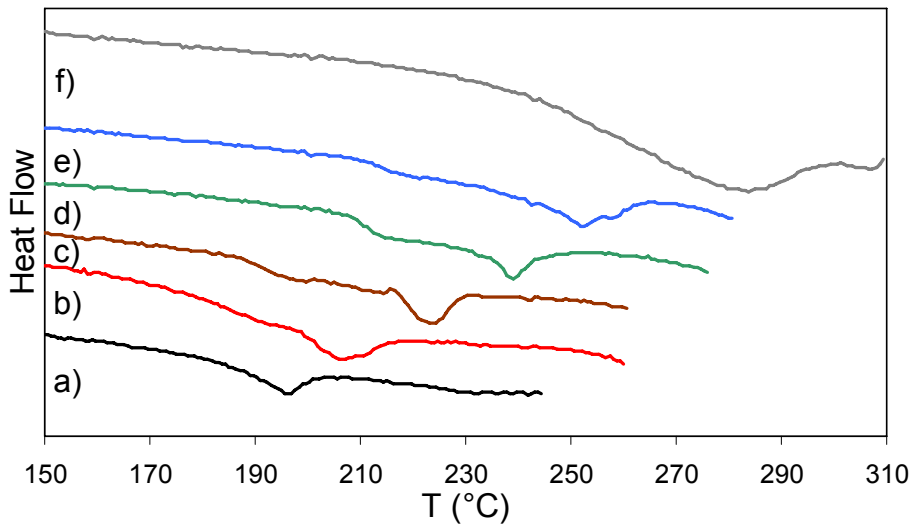

Fig. 8. DSC traces of BU-POSS copolymers at high temperature: BU-POSS 4 (- a), BU-POSS 5 (- b), BU-POSS 6 (- c), BU-POSS 7 (- d), BU-POSS 8 (- e), BU-POSS 9 (- f).

Finally, thermal stability of the hybrid methacrylic copolymers was studied through TGA experiments. It is known that incorporation of POSS nanoparticles in a polymer matrix can significantly improve its heat stability [25]. TGA results are shown in Figure 9, while it can be observed that the char yield (Table 6) substantially corresponds to the content of inorganic phase in the copolymers.

Tab. 6. Residual char at 700°C and inorganic phase content of EE-POSS copolymers.

Sample	%wt residual at 700 °C	%wt SiO
EE Homopolymer	0,0	0,0
EE-POSS 10	6,6	4,3
EE-POSS 20	7,3	8,5
EE-POSS 30	10,3	12,8
EE-POSS 40	16,8	17,2
EE-POSS 50	20,7	21,3
EE-POSS 60	22,1	25,5
EE-POSS 70	29,2	29,8
EE-POSS 80	33,5	33,9
EE-POSS 90	38,4	38,1

The observation of the DTG trends can be more interesting, since it shows the temperature of maximum degradation rate and therefore can be correlated to the degradation mechanisms. As an example Figure 10 compares the DTG curves of EE homopolymer and of POSS-based copolymer with 50%wt of silsesquioxane. For the nanostructured copolymer the maximum of degradation rate is shifted to higher temperature (around +282°C instead of +260°C).

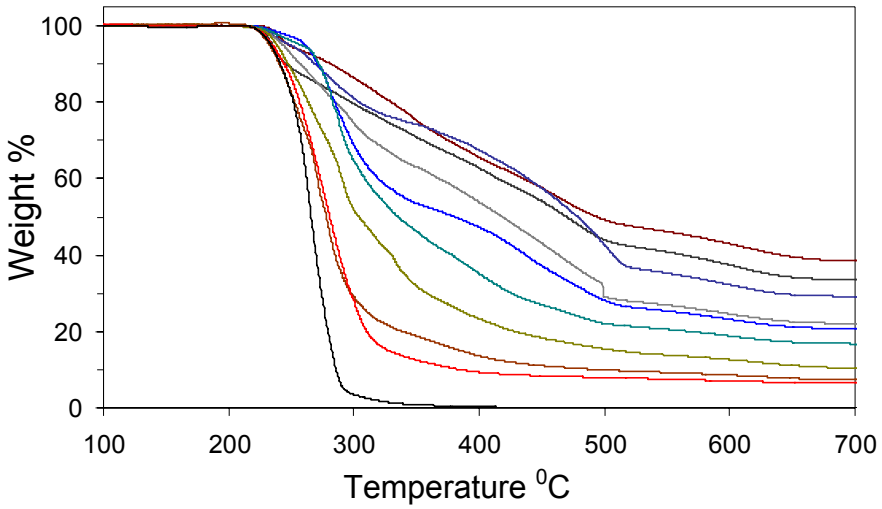

Fig. 9. Thermo-gravimetric analysis of EE-POSS copolymer series.

In addition a new degradation process at temperature above 350 °C occurs for hybrid structures. This last effect could be due to the oxidation of the POSS cage on the surface of the sample, while the phenomena observed at lower temperature can be attributed to the degradation of organic parts of copolymers. It should be noticed that samples analyzed came directly from the purification procedure, and were therefore characterized by the presence of a self-assembled nanocrystalline phase.

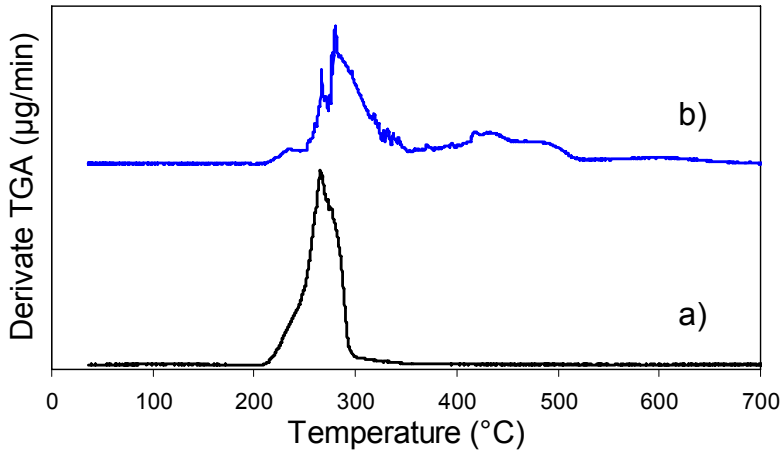

Fig. 10. DTG analysis of polybutylmethacrylate homopolymer (- a) and BU-POSS 5 copolymer (- b).

Experimental part

Starting materials

Methacrylcyclohexyl Polyhedral oligomeric silsesquioxane (POSS) was purchased from Hybrid Plastics, stored in refrigerator and used as received. Butyl methacrylate and 2-ethylhexyl methacrylate were purchased by Fluka Chemie Ag and stored in sealed bottle in a refrigerator. Azoisobutyronitrile was purchased from Fluka Chemie Ag, stored in a refrigerator and recrystallized before use. Toluene was purchased from Aldrich and distilled before use. Other solvents were purchased from J.T. Baker and used as received.

Polymerization

Poly(ethylhexylmethacrylate-co-methacrylcyclohexyl POSS) (EE-POSS) and poly (butylmethacrylate-co-methacrylcyclohexyl POSS) (BU-POSS) were prepared by a solution phase free radical polymerization process. The monomers were dissolved in toluene (50%wt) and polymerized with AIBN initiator (1%mol based on monomers) at 70 °C under a nitrogen atmosphere for 24 h. A series of EE-POSS and BU-POSS copolymers of varying POSS contents were prepared in this manner. The polymer product was then precipitated in methanol. The purification procedure of the product was carried out by reprecipitation from toluene solutions (7 g/ml) into methanol excess (14 parts), repeating the procedure at least three times. Purified copolymers were accurately oven dried *in vacuo* at 60 °C until constant weight was reached.

Characterization

Nuclear Magnetic Resonance: ^{1}H-NMR was performed in deuterated chloroform ($CDCl_3$) using a Bruker AC 300 spectrometer, working at 300.133 MHz. Calculations were made with MestRe-C software.

Gel Permeation Chromatography: GPC was carried out at +30°C using a Waters 510 pump, four Styragel columns (10^3 – 10^6 Å porosity) and a Waters 410 refractive index detector. Molecular weights obtained were relative to narrow molecular weight polymethylmethacrylate standards.

X Ray Diffractometry: XRD investigation of morphology was done with a Philips PW 1710 diffractometer, with angular range 2θ from 2 to 40° and using CuKα radiation with wavelength λ=1.5406 Å. Samples for analyses were prepared in two different ways. In the former the low POSS content copolymers were dissolved in toluene, cast in aluminium sample holders, and evaporated at ambient temperature. In the latter method the high POSS hybrids coming from polymerization were directly powderized.

Differential Scanning Calorimetry: Thermal transitions of both POSS copolymer series were investigated by DSC in heating scans at 20 °/min using a Mettler TA 3000 instrument Indium and n-hexane calibrated.

Thermo-Gravimetric Analysis: TGA was carried out with a Seiko TG/DTA 6300 instrument in air atmosphere starting from 25°C to 1000°C with a heating rate of 2°C/min.

References

[1] Schwab, J.J.; Lichtenhan, J.D. *Appl. Organometal. Chem*., **1998**, 12, 707.
[2] Shockey, E.G.; Bolf, A.G.; Jones, P.F.; Schwab, J.J.; Chaffee, K.P.; Haddad, T.S.; Lichtenhan, J.D. *Appl. Organometal. Chem*., **1999**, 13, 311.
[3] Li, G.; Wang, L.; Ni, H.; Pittman, C.U. *J. Inorg. Organometal. Polym*., **2001**, 11, 123.
[4] Phillips, H.S.; Haddad, T.S.; Tomczak, S.J. *Curr. Opin. Solid State Mater. Sci*., **2002**, 6, 205.
[5] Laine, R.M. *J. Mater. Chem*., **2005**, 15, 3725.
[6] Turri, S.; Levi, M. *Macromolecules*, **2005**, 38, 5569.
[7] Waddon, A.J.; Coughlin, E.B. *Chem. Mater*. **2003**, 15, 4555.
[8] Lichtenhan, J.D.; Otonari, Y.A.; Carr, M.J. *Macromolecules*, **1995**, 28, 8435.
[9] Romo-Uribe, A.; Mather, P.T.; Haddad, T.S.; Lichtenhan, J.D. *J. Polym. Sci.; Part B: Polym. Phys.*, **1998**, 36, 1857.
[10] Mather, P. T.; Hong, G. J.; Romo-Uribe, A.; Haddad, T. S.; Lichtenhan, J.D. *Macromolecules*, **1999**, 32, 1194.
[11] Fu, B.X.; Zhang, W.; Hsiao, B.S.; Rafailovich, M.; Solokov, J.; Johansson, G.; Sauer, B.B.; Phillips, S.; Balnski, R. *High Perform. Polym*. **2000**, 12, 565.
[12] Zheng, L.; Hong, S.; Cardoen, G.; Burgaz, E.; Gido, S.P.; Coughlin, E.B. *Macromolecules*, **2004**, 37, 8606.
[13] Waddon, A.J.; Zheng, L.; Farris, R.J.; Coughlin, E.B. *Nano Lett*., **2002**, 2, 1149.
[14] Zheng, L.; Waddon, A.J.; Farris, R.J.; Coughlin, E.B. *Macromolecules*, **2002**, 35, 2375.

[15] Pyun, J.; Matyjaszewski, K. *Macromolecules*, **2000**, 33, 217.
[16] Tegou, E.; Bellas, V.; Gogolides, E.; Argitis, P. *Microelectron. Eng*., **2004**, 73, 238.
[17] Mayo, F.R.; Lewis, F.M. *J. Am. Chem. Soc.,* **1944**, 12, 205.
[18] Fineman, R.; Ross, S.D. *J. Polym. Sci*., **1950**, 5, 259.
[19] Kelen, T.; Tudos, F. *J. Macromol. Sci., Chem*., **1975**, A9, 1.
[20] Fox, T.G. *Bull. Am. Phys. Soc*., **1956**, 1, 123.
[21] Johnston, N. W. *J. Macromol. Sci. – Rev. Macromol. Chem*., **1976**, C14 (2), 215.
[22] Couchman, P. R.; Karasz, F. E*. Macromolecules* **1978**, 11, 117.
[23] Haddad, T.S.; Lichtenhan, J.D. *Macromolecules,* **1996**, 29, 7302.
[24] Pyun, J.; Matyjaszewski, K.; Wu, J.; Kim, G.M.; Chun, S.B.; Mather, P.T.; *Polymer*, **2003**, 44, 2739.
[25] Carroll, J. B.; Waddon, A. J.; Nakade, H.; Rotello V. M. *Macromolecules*, **2003**, 35, 6289.